Growth of aligned multiwalled carbon nanotube arrays film on stainless steel substrates for electrode applications

FENGSHI CAI[a,b*], JING WANG[a], ZHIHAO YUAN[a,b], XUELI DU[a,c]

[a] *Nanomaterial & Nanotechnology Research Center, Tianjin University of Technology, Tianjin 300384, P R China*

[b] *Key Laboratory of Display Materials and Photoelectric Devices (Tianjin University of Technology), Ministry of Education of China, Tianjin 300384, P R China*

[c] *Tianjin Key Lab for Photoelectric Materials & Devices, Tianjin 300384, P R China*

The aligned multiwalled carbon nanotube (AMWCNT) films were grown on stainless steel (StS) substrates by low temperature chemical vapor deposition. Their properties and application as novel, low cost and highly efficient counter electrodes for dye sensitized solar cells (DSCs) were investigated. Due to high catalytic activity of the AMWCNT films and good conductivity of StS substrates, an overall light-to-electricity conversion efficiency of 7.03% is obtained for the DSCs based on AMWCNT/StS electrode under AM 1.5 irradiation (100 mW cm^{-2}). The stability test at moderate conditions indicated the good stability of the AMWCNT/StS electrode in the electrolyte containing iodide/triiodide. The results demonstrate a potential alternative to the expensive noble metal Pt/FTO in future applications of DSCs.

(Received February 14, 2012; accepted April 11, 2012)

Keywords: Dye-sensitized solar cells, Aligned multiwalled carbon nanotube arrays, Counter electrodes, Light-to-electricity conversion efficiency, Stainless steel substrates

1. Introduction

Dye-sensitized solar cells (DSCs) have attracted considerable interest for their potential advantages of high efficiency and low cost [1]. In the DSCs, the counter electrode plays important roles for the redox couple (I^-/I_3^-) regeneration and electron transfer [2]. At present, the counter electrodes in DSCs are usually made of the platinum on a transparent conducting oxide (TCO) glass substrate to keep high photovoltaic performances [3]. However, platinum is the precious metal in the world, and TCO glass substrate is one of the most expensive components of DSCs, thereby it is desirable to seek low-cost and Pt-free counter electrode alternatives for future development of DSCs [4,5].

Recently, various materials such as carbon-based materials [6-9] and conducting polymers [10,11] have been investigated as cost-effective and stable catalyst for I_3^- reduction to replace platinum in DSCs. Among different forms of carbon material, carbon nanotubes (CNTs) are efficient to catalyze the tri-iodide reduction and, thus, are good candidates to replace Platinum in DSCs [4, 12-15]. The catalytic activity of CNTs has been ascribed to defects of the CNT sidewalls. However, the most studied CNT based counter electrode material in the DSCs is the random network type film, prepared by spraying or spin coating on TCO glass substrates. Probably the random network structure limits the available catalytic surface area of the carbon material, and a contact problem between the CNTs and the substrate reduces the catalytic properties of the counter electrode. The aligned CNT arrays offer direct electrical pathways for the electron transport and has much higher available catalytic surface area than any random network film, which in turn may improve the performance of DSCs [16-18].To date, there are only a few reports that describe the aligned CNT arrays on TCO as a counter electrode for the efficiency improvement of DSCs [19]. On the other hand, flexible metal substrate such as stainless steel (StS) sheets has excellent electrical and thermal conductivity, making them excellent candidates as counter electrode substrate, which can reduce the sheet resistance and the manufacturing cost of DSCs [20-22]. Thus we attempted to grow one layer of aligned multiwalled carbon nanotube (AMWCNT) films directly on a StS substrate as the counter electrode by low temperature chemical vapor deposition (CVD). A light-to-electricity conversion efficiency of 7.03% was achieved for the DSCs with the AMWCNT/StS electrode, comparable with a typical Pt/fluorine-doped tin oxide (FTO) counter electrode.

2. Experimental

2.1. Preparation of aligned CNT counter electrode

The aligned CNT counter electrode was obtained by a chemical vapor deposition method to grow the CNT array directly on the surface of stainless steel 304 (1.25 mm, Outokumpu Ltd.) [14]. Briefly, the aligned CNT films were grown on StS substrates coated with a 10 nm layer of silicon and a 5 nm layer of iron as catalyst, using ethylene as a feedstock. Typical processing conditions involve flowing argon at 200 sccm, ethylene at 100 sccm, and hydrogen at 100 sccm for 5 minutes through a quartz tube heated to 700 °C.

As a comparison, the Pt counter electrodes were prepared by thermal decomposition of H_2PtCl_6 (30 mM in isopropanol) on the FTO (15Ω sq^{-1}, Nippon Sheet Glass) substrates at 385 °C for 30 min.

2.2. Preparation of TiO_2 photoanode and Solar Cell Fabrication

Nanocrystalline TiO_2 film was prepared according to the reported method [23]. The FTO glass was washed with ethanol and then treated with 50 mM $TiCl_4$ aqueous solution at 70 °C for 30 min. The TiO_2 paste (P25, Degussa AG of Germany) was printed on the pretreated FTO using a screen printing technique and then sintered in the air at 450 °C for 30 min. After cooling to room temperature, the films were treated with 50 mM $TiCl_4$ aqueous solution and recalcined at 450 °C for 30 min. The resulting film thickness was about 12 μm. Adsorption of the dyes on the TiO_2 surface was done by soaking the TiO_2 electrodes in 0.5 mM N719 dye (*cis*-bis(isothiocyanato)bis(2,2′-bipyridyl-4,4′-dicarboxylato)ruthenium(II)bistetra-butylammonium) in anhydrous ethanol at room temperature for 24 h.

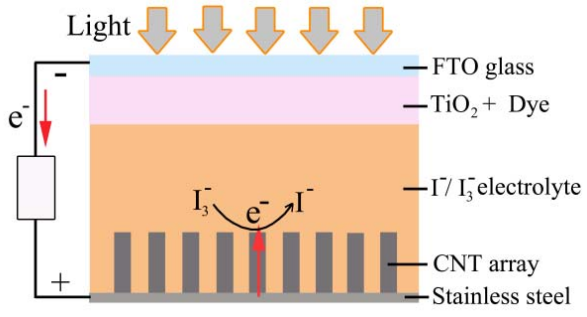

Fig. 1. Schematic image of the dye-sensitized solar cells with the TiO_2 photoanode and the AMWCNT counter electrode. The AMWCNT provides a direct path for the electron exchange.

DSCs were assembled by injecting the electrolyte into the aperture between the dye-sensitized nanoporous TiO_2 photoanode and the counter electrode, as shown in Fig. 1. The electrolyte was a mixture of 0.6 M of 1-butyl-3-methylimidazolium iodide (BMImI), 0.03 M of iodine, 0.1 M guanidine thiocyanate and 0.5 M of 4-tert-butylpyridine in acetonitrile. Surlyn 1702 (60 μm thick) was used as the spacer between the two electrodes. The electrolyte was inserted into the cell by means of vacuum backfilling through a hole on the side of counter electrode. Then the hole was sealed by using glass cement and a cover glass (1mm thick) at room temperature. The effective area of the cells was 0.16 cm^2.

2.3. Characterization and measurements

The morphologies and microstructures of the CNTs films were characterized by scanning electron microscope (SEM, JEOL, JSM-6700F, 10 kV) and transmission electron microscope (TEM, JEOL, JEM-2100, 200 kV). The Raman spectra were collected by using a mirco-Raman spectrometer with 514-nm (argon ion) wavelength laser probe.

The photocurrent (I) –voltage (V) characteristics of DSCs were measured by a Keithley 2400 digital source meter controlled by a computer. An AM1.5 solar simulator -Oriel 91160–1000 with a 300 W Xe lamp was used as the light source. The incident-light intensity was calibrated to 100 mW cm^{-2} using a standard single-crystal Si solar cell. The light-to-electricity conversion efficiency (η) of the DSCs is calculated from the short-circuit photocurrent density (J_{sc}), the open-circuit photovoltage (V_{oc}), the fill factor of the cell (*ff*), and the intensity of the incident light (I_s) by the following equation [24]:

$$\eta = \frac{J_{sc}\, V_{oc}\, \mathrm{ff}}{I_s}$$

The electrochemical performance was investigated by means of a PARSTAT 2273 instrument at open-circuit potential under AM 1.5 one sun light illumination, with frequency range of 0.01–10^5 Hz. The magnitude of the alternative signal was 10 mV. The electrical impedance spectra were analyzed using Z-View software.

3. Results and discussion

Fig. 2a, b show a typical SEM image of the as-prepared CNTs grown on stainless steel substrate, displaying a highly uniform and well-spaced arrays character with the CNTs length of about 2 μm. The average tube-to-tube spacing between the nanotubes within the film is ~30 nm. The CNTs grown directly on the StS substrate shows better contact with the StS surface, and avoids the bonding effects of CNTs without any degradation of the surface. The detailed morphology and microstructure of the CNTs is further characterized by TEM (Fig. 2c). It is observed that the hollow nanotube has an outer diameter of about 20 nm and the

defect-rich multiwall tube surface with discontinuous graphite layers, which is marked with white arrows. The defect-rich edge-planes of the MWCNTs provide a large number of active sites for redox reactions at the counter electrode/electrolyte interface [13]. Another evidence for the presence of defect-rich in MWCNTs comes from the Raman spectrum shown in Fig. 2d. The D (disorder mode) band at 1350 cm^{-1} is characteristic of defects or the finite size of the nanotubes, while the G (graphite) band at 1583 cm^{-1} is attributed to the E_{2g} vibrational mode of graphite layers [25]. The existence of D-band with considerable peak intensity indicates that there are many disordered or amorphous parts in the structure of the obtained MWCNTs, being consistent with the TEM images in Fig. 2c. The intensity ratio of the D-band to G-band is about 1.14, demonstrating that the obtained MWCNTs are partially composed of graphite structures [26].

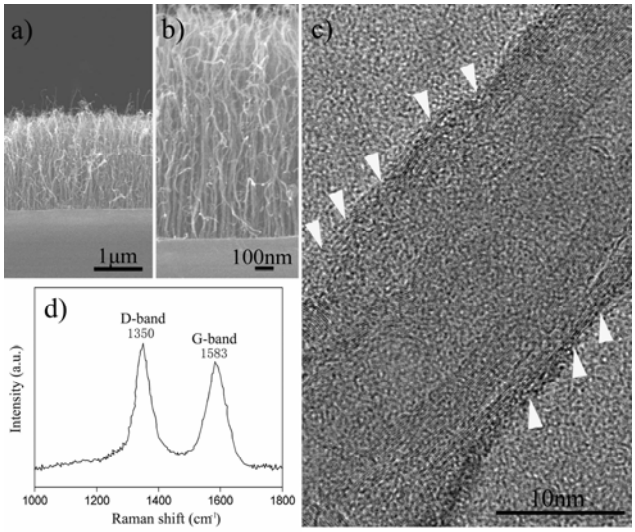

Fig. 2. (a), (b) SEM image of cross section of the as-prepared CNT array film on a stainless steel substrate. (c) TEM image of the as-prepared CNT. White arrows represent surface defects of discontinuous graphite layers. (d) Raman spectrum of the CNT.

Fig. 3 shows *I-V* characteristic curves of the DSCs with different counter electrodes of AMWCNT/StS, Pt/FTO, and bare StS. The detailed photovoltaic parameters (J_{sc}, V_{oc}, *ff*, η) are summarized in Table 1. It can be seen that the DSCs with typical Pt/FTO electrodes have the following photovoltaic parameters: V_{oc} = 0.720 V, J_{sc} = 15.19 mA cm^{-2}, *ff* = 0.62, and η = 6.78%. For the AMWCNT/StS electrode, the photovoltaic parameters, V_{oc}, J_{sc}, *ff*, and η are 0.712 V, 15.43 mA cm^{-2}, 0.64, and 7.03%, respectively. Obviously, the V_{oc} and J_{sc} of the DSCs with the AMWCNT/StS are very close to those of the DSCs using Pt/FTO, while the *ff* and η are slightly higher than that of the DSCs based on Pt/FTO. As a reference, the DSCs with a bare StS substrate as a counter electrode has a poor η of 0.08% due to poor electrocatalytic activity for reduction of triiodide. In general, the AMWCNT/StS presents an excellent photovoltaic performance, comparable with Pt/FTO electrode.

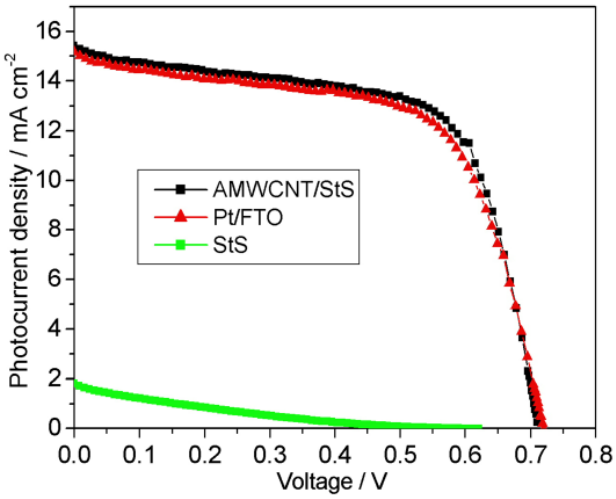

Fig. 3. Photocurrent (I)–voltage (V) curves of DSCs with AMWCNT/StS, Pt/FTO, and bare StS counter electrodes, measured under simulated sunlight of AM 1.5–100mW cm^{-2}.

Table 1. Photovoltaic Parameters of DSCs in Fig. 3.

Counter electrode	V_{oc}(V)	J_{sc} (mA cm^{-2})	*ff*	η (%)
AMWCNT/StS	0.712	15.43	0.64	7.03
Pt/FTO	0.720	15.19	0.62	6.78
StS	0.615	1.82	0.07	0.08

To evaluate the catalytic performance of the AMWCNT/StS counter electrode in DSCs, electrochemical impedance spectra (EIS) were measured. Fig. 4 shows the Nyquist plots of the thin-layer symmetric cells with two identical AMWCNT/StS or Pt/FTO counter electrodes fitted with the equivalent circuit (inset in Fig. 4). Two semicircles were observed in the measured frequency range of 0.01–10^5 Hz. The semicircle in the high-frequency region corresponds to the charge-transfer resistance (R_{ct}) of the counter electrode/electrolyte interface, and the one in the low-frequency region represents the Nernstian diffusion of the I^-/I_3^- redox species in the electrolyte [23]. The fitted electrochemical parameters from EIS are summarized in Table 2.

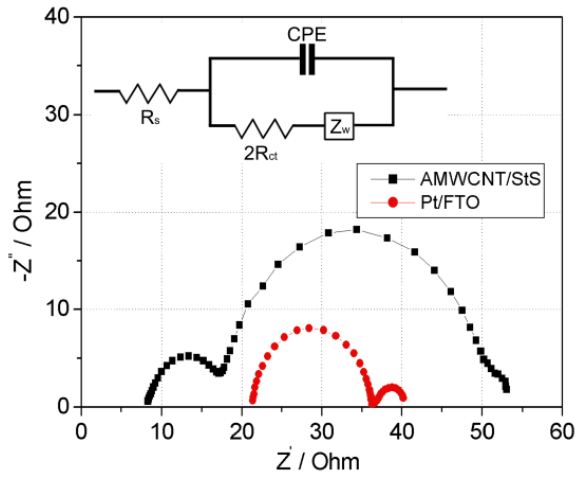

Fig. 4. Nyquist plots of the symmetric cells with two identical counter electrodes of AMWCNT/StS or FTO/Pt with a distance of 60 μm. The inset is equivalent circuit of EIS. R_s: ohmic serial resistance; CPE: constant phase element; R_{CT}: charge-transfer resistance; Z_W: Nernst diffusion impedance.

Table 2. Impedance parameters of the various counter electrodes estimated from the impedance spectra in Fig. 4.

CE	R_s (Ω)	CPE-T (F)	R_{CT} (Ω)
AMWCNT/StS	8.26	5.13×10^{-3}	4.68
Pt/FTO	21.39	9.27×10^{-5}	7.75

Clearly, the R_{ct} of the AMWCNT/StS electrode is 4.68 Ω which is slightly lower than the value of 7.75 Ω for the Pt/FTO electrode. This indicates that the AMWCNTs have a superior electrocatalytic activity for the redox reaction of the I^-/I_3^- couple. The ohmic internal resistance of AMWCNT/StS (8.26 Ω) is much lower than that of the typical FTO/Pt electrode (21.39 Ω), as expected due to the good electrical conductivity of CNTs arrays and the difference in the sheet resistance between the StS substrate and the FTO substrate. The simulated chemical capacitance (5.13×10^{-3} F) of the CNTs arrays electrode is obviously larger than that of the FTO/Pt electrode (9.27×10^{-5} F), demonstrating the high active surface area and corresponding chemical capacitance charging/discharging characteristics at the porous electrode/electrolyte interface [27]. Therefore, the use of the as-prepared CNTs arrays/StS as counter electrodes can not only reduce charge-transfer resistances and ohmic internal resistances, but also provide an efficient electron transition channel along the CNTs, resulting in good photovoltaic performance.

To further examine the stability of cell performance of DSCs based on AMWCNT/StS, we carried out the decay test. Fig. 5 shows the variation in the current-voltage parameters of sealed devices stored in dark at room temperature. The V_{oc} and *ff* were enhanced moderately from 0.71 to 0.72 V and 0.64 to 0.67, respectively; while the J_{sc} decreased by 7.7% and η was no notable change on the whole. This result suggests that the AMWCNT/StS is relatively stable in the liquid electrolyte containing I^-/I_3^- redox couples.

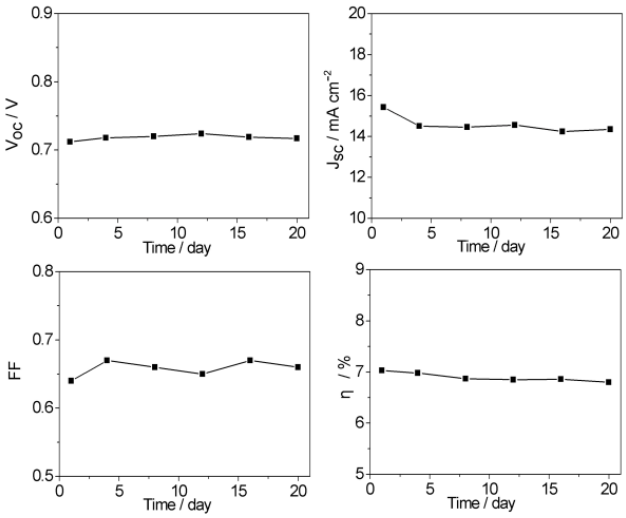

Fig. 5. Variation of photovoltaic parameters of sealed DSCs based on AMWCNT/StS under one sun illumination (AM 1.5, 100 mW cm^{-2}).

4. Conclusions

In summary, aligned multiwalled carbon nanotube films on StS substrates have been synthesized and successfully used as counter electrodes in DSCs. Electrochemical measurements show that the defect-rich AMWCNT films result in low charge-transfer resistance at the counter electrode/electrolyte interfaces, and an introduction of the StS substrate reduce ohmic internal resistances of DSCs. A light-to-electricity conversion efficiency of 7.03% is achieved for the DSCs with the AMWCNT/StS electrode. The stability test at moderate conditions confirms that AMWCNT/StS can be readily used as counter electrodes in DSCs. Thus we believe that this work is promising in the area of replacing Pt/FTO for the application in DSCs.

Acknowledgements

This work was supported by the National NSFC (20903073, 50872092) and Tianjin Natural Science Foundation (09JCYBJC07000).

References

[1] B. O'Regan, M. Grätzel, Nature **353**, 737 (1991).
[2] N. Papageorgiou,W. F. Maier, M. Grätzel, J. Electrochem. Soc. **144**, 876 (1997).
[3] T. N. Murakami, M. Grätzel, Inorg. Chim. Acta **361**, 572 (2008).
[4] G. Calogero, F. Bonaccorso, O. M. Marago, P. G. Gucciardi, G. Di Marco, Dalton Trans. **39**, 2903 (2010).
[5] A. Kanciurzewska, E. Dobruchowska, A. Baranzahi, E. Carlegrim, M. Fahlman, M. A. Girtu, J. Optoelectron. Adv. Mater. **9**, 1052 (2007).
[6] T. N. Murakami, S. Ito, Q.Wang, M.K. Nazeeruddin, T. Bessho, I. Cesar, P. Liska, R. Humphry-Baker, P. Comte, P. P´echy, M. Grätzel, J. Electrochem. Soc. **153**, A2255 (2006).
[7] K. Imoto, K. Takatashi, T.Yamaguchi, T.Komura, J. Nakamura, K. Murata, Sol. Energy Mater. Sol. Cells **79**, 459 (2003).
[8] Z. Huang, X. Z. Liu, K. X. Li, D. M. Li, Y. H. Luo, H. Li, W. B. Song, L. Q. Chen, Q. B. Meng, Electrochem. Commun. **9**, 596 (2007).
[9] T. Hino, Y. Ogawa, N. Kuramoto, Carbon **44**, 880 (2006).
[10] J. B. Xia, N. Masaki, K. J. Jiang, S. Yanagida, J. Mater. Chem. **17**, 2845 (2007).
[11] J. H. Wu, Q. H. Li, L. Q. Fan, Z. Lan, P. J. Li, J. M. Lin, S. C. Hao, J. Power Sources **181**, 172 (2008).
[12] K. Suzuki, M.Yamaguchi, M.Kumagai, S.Yanagida, Chem. Lett. **32**, 28 (2003).
[13] W. J. Lee, E. Ramasamy, D. Y. Lee, J. S. Song, ACS Appl. Mater. Interfaces **1**,145 (2009).
[14] J. E. Trancik, S. C. Barton, J. Hone, Nano Lett. **8**, 982 (2008).
[15] K. Aitola, J. Halme, N. Halonen, A. Kaskela, M. Toivola, A. G. Nasibulin, K. Kordás, G. Tóth, E. I. Kauppinen, P. D. Lund, Thin Solid Films **519**, 8125 (2011).
[16] P. Dong, C. L. Pint, M. Hainey, F. Mirri, Y. J. Zhan, J. Zhang, M. Pasquali, R. H. Hauge, R. Verduzco, M. Jiang, H. Lin, J. Lou, ACS Appl. Mater. Interfaces **3**, 3157 (2011).
[17] H. W. Zhu, H. F. Zeng, V. Subramanian, C. Masarapu, K. H. Hung, B. Q. Wei, Nanotechnology, **19**, 465204 (2008).
[18] K. S. Lee, W. J. Lee, N. G. Park, S. O. Kim, J. H. Park, Chem. Commun. **47**, 4264 (2011).
[19] Z. B. Yang, T. Chen, R. X. He, G. Z. Guan, H. P. Li, L. B. Qiu, H. S. Peng, Adv. Mater. **23**, 5436 (2011).
[20] K. Miettunen, J. Halme, M. Toivola, P. Lund, J. Phys. Chem. C **112**, 4011 (2008).
[21] T. Ma, X. Fang, M. Akiyama, K. Inoue, H. Noma, E. Abe, J. Electroanal. Chem. **574**, 77 (2004).
[22] M. G. Kang, N.-G. Park, K. S. Ryu, S. H. Chang, K.-J. Kim, Sol. Energy Mater. Sol. Cells **90**, 574 (2006).
[23] F. S. Cai, J. Liang, Z. L. Tao, J. Chen, R. S. Xu, J. Power Sources **177**, 631 (2008).
[24] A. Hagfeldt, M. Grätzel, Acc. Chem. Res. **33**, 269 (2000).
[25] C. Thomsen, Phys. Rev. B **61**, 4542 (2000).
[26] R. A. DiLeo, B. J. Landi, R. P. Raffaelle, J. Appl. Phys. **101**, 064307 (2007).
[27] J. Bisquert, M. Grätzel, Q. Wang, F. Fabregat-Santiago, J. Phys. Chem. B **110**, 11284 (2006).

*Corresponding author: caifs@tjut.edu.cn